

Spatio-temporal variability of zooplankton standing stock in eastern Arabian Sea inferred from ADCP backscatter measurements

Ranjan Kumar Sahu, P. Amol, D.V. Desai, S.G. Aparna, D. Shankar

May 14, 2024

Abstract

We use acoustic Doppler current profiler (ADCP) backscatter measurements to map the spatio-temporal variation of zooplankton standing stock in the eastern Arabian Sea (EAS). The ADCP moorings were deployed at seven locations on the continental slope off the west coast of India; we use data from October 2017 to December 2023. The 153.3 kHz ADCP uses backscatter from sediments or organisms such as copepods, ctenophores, salps and amphipods greater than 1 cm to calculate current profile. The backscatter is obtained from echo intensity using RSSI conversion factor after doing necessary calibrations. The conversion from backscatter to biomass is based on volumetric zooplankton sampling at the respective locations. Analysis of the data over 25 – 140 m shows that the backscatter and zooplankton biomass decrease from the upper ocean (215 m g^{-3} biomass contour) to the lower depths. Changes are observed in the seasonal variation of the monthly

¹² climatology of zooplankton standing stock (integral of the biomass over 20 – 140 m water column)
¹³ as we move to poleward along the slope in EAS. The range of variation of standing stock is lowest
¹⁴ at Kanyakumari, followed by Okha, which lie at the southern and northern boundary of the EAS,
¹⁵ respectively. Complementary variables are used to explain the processes leading to growth or decay
¹⁶ of zooplankton biomass.

₁₇ **1 Introduction**

₁₈ **1.1 Background**

₁₉ Zooplankton plays a vital role in food web of pelagic ecosystem by enabling the hierarchical trans-
₂₀ port of organic matter from primary producers to higher trophic levels impacting the fish population
₂₁ and the carbon pump of the deep ocean [Ohman and Hirche, 2001, Le Qu et al., 2016]. They are
₂₂ presumably the largest migrating organisms in terms of biomass [Hays, 2003] which occurs in Diel
₂₃ Vertical Migration (DVM). Zooplanktons depend not only on phytoplankton but other environ-
₂₄ mental parameters (e.g. Mixed layer depth, insolation, Oxygen, thermocline, nutrient availability,
₂₅ chlorophyll concentration and daily primary production). The biological productivity of the ocean
₂₆ is essentially connected with physics and chemistry [Subrahmanyam, 1959, Ryther et al., 1966,
₂₇ Qasim, 1977, Nair, 1970, Banse, 1995, McCreary et al., 2009, Vijith et al., 2016, Amol et al., 2020].
₂₈ The dynamic ocean results in varying physico-chemical properties, leading to bloom and growth of
₂₉ planktons in favourable conditions. The changes are strongly influenced by the seasonal cycle in
₃₀ the North Indian Ocean (NIO; north of 5 °N of Indian Ocean). The eastern boundary of Arabian
₃₁ Sea contains the West India Coastal Current (WICC; [Patil et al., 1964, Ramamirtham and Murty,
₃₂ 1965, Banse, 1968, Shetye et al., 1991, McCreary Jr et al., 1993, Shankar and Shetye, 1997, Shetye
₃₃ and Gouveia, 1998, Maheswaran et al., 2000, Amol et al., 2014, Chaudhuri et al., 2020, 2021])
₃₄ which reverses seasonally, flowing poleward (equator-ward) during November to February (June to
₃₅ September).
₃₆ The direct consequence of this reversal is the seasonal cycle of thermocline, oxycline and thick-
₃₇ ness of mixed Layer Depth (MLD) induced by upwelling favourable conditions in summer and down-
₃₈ welling favourable conditions in winter in eastern Arabian Sea (EAS). Further, the phytoplankton

39 biomass and chlorophyll concentration changes with the season [Subrahmanyam and Sarma, 1960,
40 Banse, 1968, Lévy et al., 2007, Vijith et al., 2016]. Upwelling in summer monsoon leads to maxi-
41 mum chlorophyll growth in the entire EAS [Banse, 1968, Banse and English, 2000, McCreary et al.,
42 2009, Hood et al., 2017]. During winter monsoon, the convective mixing induced winter mixed layer
43 [Shetye et al., 1992, Madhupratap et al., 1996b, Lévy et al., 2007, Vijith et al., 2016, Shankar et al.,
44 2016, Keerthi et al., 2017] results in winter chlorophyll peak in northern EAS (NEAS) while the
45 downwelling Rossby waves modulate chlorophyll along the southern EAS (SEAS) albeit limited to
46 coast and islands [Amol et al., 2020]. (For a detailed description on EAS division, please refer figure
47 1 of [Shankar et al., 2019].

48 The zooplankton grazing peak is instantaneous with no time delay from peak phytoplankton
49 production [Li et al., 2000], but its population growth lags [Rehim and Imran, 2012, Almén and
50 Tamelander, 2020] depending on its gestation period and other limiting aspects. While some studies
51 suggest that the peak timing of zooplankton may not change in parallel with phytoplankton blooms
52 [Winder and Schindler, 2004], others indicate that lag exists between primary production and the
53 transfer of energy to higher trophic levels [Brock and McClain, 1992, Brock et al., 1991]. A recent
54 work [Aparna et al., 2022] had shown that peak zooplankton population may never occur even
55 with a bloom in phytoplankton such as in SEAS, leading to the collapse of ecological models and
56 succeeding food webs of higher trophic levels.

57 The conventional zooplankton measurements, where only few snapshot/s of the event is cap-
58 tured gives an incoherent or incomplete understanding in terms of spatio-temporal variation of
59 zooplankton [Ramamurthy, 1965, Piontkovski et al., 1995, Madhupratap et al., 1992, 1996a, Wish-
60 ner et al., 1998] as much information is revealed by later studies [Jyothibabu et al., 2010, Vijith
61 et al., 2016, Shankar et al., 2019, Aparna et al., 2022] using high resolution data. Calibrated acous-

tic instruments such as Acoustic Doppler Current Profiler (ADCP) along with relevant data can be utilised to understand small scale variability [Nair et al., 1999, Edvardsen et al., 2003, Smith and Madhupratap, 2005, Smeti et al., 2015, Kang et al., 2024], the complex interplay between the physico-chemical parameters and ecosystem [Jiang et al., 2007, Potiris et al., 2018, Shankar et al., 2019, Aparna et al., 2022, Nie et al., 2023], the zooplankton migration [Inoue et al., 2016, Ursella et al., 2018, 2021] and their seasonal to annual variation [Jiang et al., 2007, Hobbs et al., 2021, Liu et al., 2022, Aparna et al., 2022].

69 1.2 ADCP backscatter and zooplankton biomass

70 At present, there are two types of acoustic samplers: non-calibrated single frequency acoustic profiler such as ADCP or calibrated multi and mono frequency acoustic profilers such as zooplankton acoustic profiler (ZAP) and Tracor acoustic profiling system(TAPS). The use of acoustics as a proxy for zooplankton biomass estimation can be traced to [Pieper, 1971, Sameoto and Paulowich, 1977] and earlier studies which used echograms to approximate the large-scale horizontal extents [Barraclough et al., 1969], and small scale vertical extent [McNaught, 1968]. The relationship between backscatter and the abundance and size of zooplankton was described by [Greenlaw, 1979] wherein it was pointed out that single frequency backscatter can be used to estimate abundance if mean zooplankton size is known. This paved the way for use of single frequency acoustic profiler. A drastic increase in study temporal and spatial variation of zooplankton biomass using backscatter-proxy came in 1990s by introduction of high frequency echo sounders, with studies [Flagg and Smith, 1989, Wiebe et al., 1990, Batchelder et al., 1995, Greene et al., 1998, Rippeth and Simpson, 1998] methodically showing acoustic backscatter estimated zooplankton biomass in various shelf and slope locations around North Atlantic, North pacific location. The foundation for further research that

84 investigated the potential of acoustic backscatter from ADCPs and multi frequency echo sounders
85 in assessing zooplankton biomass and comprehending zooplankton dynamics in diverse maritime
86 habitats was established by these initial explorative experiments.

87 Acoustic backscatter and zooplankton biomass have been better understood as a result of tech-
88 nological and methodological developments over time. Net sampling augmented ADCP backscatter
89 have been used to study DVM and the spatial and temporal variability of zooplankton biomass by
90 [Cisewski et al., 2010, Smeti et al., 2015, Guerra et al., 2019] in different marine regions, such as the
91 Southwestern Pacific, the Lazarev Sea in Antarctica and the Corsica Channel in the north-western
92 Mediterranean Sea. The zooplankton biomass variation in the Arabian sea has been studied during
93 JGOFS programme in 1990s [Herring et al., 1998, Nair et al., 1999, Fielding et al., 2004, Smith and
94 Madhupratap, 2005]. However, their studies were limited to the cruise duration as vessel mounted
95 ADCPs were predominantly used; hence long-term data was sparsely produced. The first such
96 study to fully exploit the immense potential of ADCPs in EAS was carried out by [Aparna et al.,
97 2022] using ADCP moorings deployed on continental slopes off the Indian west coasts [Amol et al.,
98 2014, Chaudhuri et al., 2020].

99 1.3 Objective and scope of the manuscript

100 A network of ADCPs has been installed off the continental slope and shelf on the west coast of
101 India. This ADCPs have enabled a rigorous view of intraseasonal to seasonal scale variability [Amol
102 et al., 2014, Chaudhuri et al., 2020]. Initially a network of 4 ADCPs (off Mumbai, Goa, Kollam and
103 Kanyakumari) on continental slope, it has been extended to include 3 more moorings (off Okha from
104 2018, Jaigarh and Udupi from 2017). In the recent study [Aparna et al., 2022] have used ADCP
105 moorings off Mumbai, Goa and Kollam to explain the temporal variability of zooplankton biomass.

106 The study showed that the zooplankton peaks (and troughs) is not only non-uniform in latitude but
107 also heavily influenced by the oxygen minimum zone, MLD and the seasonal upwelling/downwelling
108 conditions. Stark contrast in the phytoplankton bloom and subsequence growth of zooplankton or
109 the lack thereof was observed in the EAS regimes.

110 We build upon the existing work by extending to include the newly incorporated ADCPs so as to
111 have a better understanding in the latitudinal variation of zooplankton biomass in EAS. The paper
112 is organized as follows; datasets and methods employed are described in detail in Section 2. Section
113 3 describes the observed seasonal cycle of zooplankton biomass and standing stock. The role of
114 mixed layer depth, net primary production, sea surface temperature, wind forcing and circulation
115 in determining the biomass is discussed in results section 4, with conclusion in section 5.

116 2 Data and methods

117 The backscatter data from ADCP and the zooplankton samples collected from the periphery of
118 mooring is described in this section. The methodology followed in processing ADCP data and
119 estimation of backscatter and subsequently the zooplankton biomass is discussed. The backscatter
120 derived from the echo intensity of the seven ADCP mooring deployed on the continental slope off
121 the Indian west coast is the primary data we have use in this manuscript. The moorings details
122 are summarised in Table1. In situ biomass data from volumetric zooplankton samples are used
123 to validate and correlate with backscatter. In addition, we have used the monthly climatology of
124 temperature and salinity [Chatterjee et al., 2012] and the net primary productivity from MODIS
125 (Moderate Resolution Imaging Spectroradiometer) and VIIRS (Visible Infrared Imaging Radiome-
126 ter Suite) from global NPP estimates (<http://sites.science.oregonstate.edu/ocean.productivity>).

127 **2.1 ADCP data and Backscatter estimation**

128 The ADCPs were deployed on the continental slope off the Indian west coast. Initially a set of
129 three ADCPs, it was gradually extended to four more sites to cover the entire EAS basin from
130 Okha (22.26°N) in north to Kanyakumari (6.96°N) in south. The moorings are serviced on yearly
131 basis usually during October-November or in winter monsoon months. The ADCPs are of RD
132 Instruments make, upward-looking and operate at 153.3 kHz. While utmost care is taken to position
133 the instrument at ~ 200 m depth, yet for some deployments it's shallow or deeper owing to drift
134 caused by floater buoyancy - anchor weight balance. Data was collected at hourly interval and the
135 bin size was set to 4 m. The echoes at surface to 10 % range (20 m) means the data at these is
136 rendered useless and is discarded from further use.

137 The procedure followed in processing of the ADCP data are described in [Amol et al., 2014]
138 and [Mukherjee et al., 2014]. An addition to their methodology was to do depth correction to ac-
139 commodate the vertical movement of ADCP buoys [Chaudhuri et al., 2020, Mukhopadhyay et al.,
140 2020] using data from pressure sensor mounted on the instrument. We have followed the method-
141 ology laid down in [Aparna et al., 2022] to derive the backscatter time series from ADCP echo
142 intensity data which is discussed later paragraph. The gaps are filled using the grafting method of
143 [Mukhopadhyay et al., 2020] once the zooplankton biomass time series is constructed.

144 The primary objective of ADCP usage is to obtain vertical current profile at a point location. It
145 is achieved by using the echo intensity received at the ADCP transducer. The instrument sensors
146 doesn't directly give backscatter, as echo intensity is range independent. Range correction has to
147 be performed before echo intensity (E) is converted to Backscatter (B). Received signal strength
148 indicator (RSSI), also called the conversion factor (Kc) which is specific to a sensor is used along with
149 the corresponding reference echo intensity (Er). It's important to state that for the same device Kc

150 remains unchanged while E_r varies over each subsequent deployment. The backscattering strength
151 (in dB) is given by [Mullison, 2017]:

$$\small{152} \quad B = [C - L_{DBM} - P_{DBW}] + 2\alpha R + 10\log_{10}[(T_{TD} + 273.16)R^2] + 10\log_{10}[10^{K_c(E-E_r)/10} - 1]$$

153 where C is an empirical constant, L_{DBM} is $10\log_{10}L$ where L is the transmit pulse length in
154 meters, P_{DBW} is $10\log_{10}P$ (P is transmitted power in watts), α is the sound absorption coefficient
155 of water (in $dB m^{-1}$), T_{TD} is the temperature (in $^{\circ} C$) at the depth of positioned instrument, R
156 is the slant range (in meters) from transducer to the scatterers and E_r is the reference level of E
157 taken in real-time (unit counts). E_r in our case is taken from first (last) measured profile when the
158 instrument is in air before (after) deployment (retrieval). The backscattering strength is referenced
159 to $(4\pi m^{-1})$ [Deines, 1999, Mullison, 2017]. Aparna et al. [2022] has discussed the relevance of each
160 of the term to the total backscattering strength. Our analysis also suggests that the α does not
161 affect the final results.

162 2.2 Zooplankton data and estimation of biomass

163 The zooplankton samples were collected in the vicinity (~ 10 km) of ADCP mooring site twice; once
164 prior retrieval and again post deployment of moorings so that there is overlap in the ADCP time
165 instance and in situ zooplankton samples. The sampling is done at the mooring location during
166 servicing cruises on board RV Sindhu Sankalp and RV Sindhu Sadhana (Table 2). Multi-plankton
167 net (MPN) ($100 \mu m$ mesh size, $0.5 m^2$ mouth area) was used to get samples in the pre-determined
168 depth ranges; water volume filtered was calculated by the product of sampling depth range and
169 the mouth area of net. The depth range and timing of sample collection was different throughout
170 the MPN hauls. From 2020 onwards, the depth-range was standardised to the bins of 0 - 25, 25 -
171 50, 50 - 75, 75 - 100, 100 - 150 (units are in meters). The collected zooplankton samples were then

¹⁷² preserved in 5 % formaldehyde solution until it's transferred to laboratory. To measure zooplankton
¹⁷³ wet weight accurately, the gelatinous forms/salps were separated. [Aparna et al., 2022] had reposted
¹⁷⁴ the calanoid copepods, cyclopoid copepods, Poecilostomatoida, Harpacticoida, appendicularians,
¹⁷⁵ euphausiids, ostracods, and chaetognaths as the major groups of zooplankton contributing to
¹⁷⁶ the biomass of net samples from the mooring sites this has to be updated to include later samples.
¹⁷⁷ The backscatter obtained earlier is averaged in vertical corresponding to the specific MPN hauls for
¹⁷⁸ each site. The backscatter is linear regressed with respective biomass to establish their relationship,
¹⁷⁹ which has been demonstrated in numerous previous studies [Flagg and Smith, 1989, Heywood et al.,
¹⁸⁰ 1991, Jiang et al., 2007, Aparna et al., 2022].

¹⁸¹ We calculated the regression equation to be $y = 0.0203 x + 4.01$ and, which is well within the
¹⁸² error range of the regression equation of [Aparna et al., 2022], $y = (0.02 \pm 0.004) x + (4.14 \pm 0.36)$
¹⁸³ with a correlation of 0.53. The correlation value in our case is 0.54; the minor difference is due to
¹⁸⁴ higher number of data points (159) in the present study.

¹⁸⁵ 2.3 Biomass time series and estimation of standing stock

¹⁸⁶ The zooplankton biomass time series is created from the above derived linear relationship: $\log_{10}(\text{biomass})$
¹⁸⁷ $= m * \text{Backscatter} + k$, where m is slope and k is intercept. The time series shows the pattern
¹⁸⁸ of diel vertical migration (DVM) at all the mooring sites during dawn (\sim 0600-0700 hours) and
¹⁸⁹ dusk (\sim 1800-1900 hours). It is evident in earlier studies using backscatter [Ashjian et al., 2002,
¹⁹⁰ Smith and Madhupratap, 2005, Inoue et al., 2016, Ursella et al., 2018] and in situ zooplankton data
¹⁹¹ [Padmavati et al., 1998]. The implication of DVM is a higher biomass at surface during the night
¹⁹² as zooplankton feeds and a lower biomass at daytime as they descend to subsurface depths. The
¹⁹³ overall biomass over the time period of a day may vary but the DVM doesn't affect the seasonal

¹⁹⁴ variation as shown by ([[Jiang et al., 2007](#), [Aparna et al., 2022](#)]). Since our goal is to study the
¹⁹⁵ seasonal variation, delineating the daily biomass is sufficient. The biomass time series is discussed
¹⁹⁶ in section **name the section**.

¹⁹⁷ The standing stock is determined by taking the depth integral of biomass. To maintain the
¹⁹⁸ consistency of standing stock estimation, only those deployments that doesn't lack data at any
¹⁹⁹ depth in the entire range of 24 - 120 m are considered for analysis. The lack of data in the above
²⁰⁰ mentioned depth range is due to deviation in positioning of ADCP sensor in the water column. A
²⁰¹ swift alteration in bathymetry along the continental slope implies that the mooring might anchor
²⁰² at a different depth than planned, hence a change in the predicted position of ADCP. This leads
²⁰³ to gap in data at few mooring sites for some year. For example, for the northern-most mooring at
²⁰⁴ Okha, data is not available for the entire upper 120 m depth for the second deployment. Also at
²⁰⁵ Jaigarh, where the surface to ~60m data (in 3rd deployment) and Kollam, where 80 m and below
²⁰⁶ (in 4th deployment) is unavailable and hence discarded from standing stock estimation. There
²⁰⁷ are few deployments where no data or bad data was recorded e.g, at Udupi (4th deployment) and
²⁰⁸ Kanyakumari (6th deployment). The seasonal cycle of standing stock for 24 - 120 m available data
²⁰⁹ is explored in section **name of the section**.

²¹⁰ 2.4 Chlorophyll and net primary productivity data

²¹¹ Previous study based on ADCP data of EAS [[Aparna et al., 2022](#)] have used SeaWiFS based
²¹² chlorophyll data for comparison with climatology of zooplankton standing stock. The SeaWiFS
²¹³ was at its end of service in 2010, hence we use new chlorophyll product. The present study has been
²¹⁴ conducted using Global Ocean Colour, biogeochemical, L3 data obtained from the [E.U. Copernicus](#)
²¹⁵ [Marine Service Information](#). The daily data is available at a spatial resolution of 4 km.

216 While chlorophyll is used to compare with the variation in climatology of zooplankton standing;
217 the growth efficiencies of zooplankton are directly linked to primary production levels, emphasizing
218 the interconnectedness between primary producers and consumers in marine food webs [Friedland
219 et al., 2012]. In their study, [Aparna et al., 2022] has emphasised on the collapse of the predator-
220 prey relationship between zooplankton-phytoplankton using climatological data. We showcase their
221 interdependency or the lack thereof using net primary productivity models. Moderate Resolution
222 Imaging Spectroradiometer (MODIS) based net primary productivity (NPP) data at a resolution
223 of $0.16^{\circ} \times 0.16^{\circ}$ was obtained from Oregon State University. They have employed three different
224 schemes to obtain NPP from Chlorophyll concentration. Those are discussed below in brief. The
225 first is Vertically Generalized Production Model (VGPM). The NPP (a rate term) is to be derived
226 from chlorophyll (a standing stock) using chlorophyll-specific assimilation efficiency for carbon fix-
227 ation. The single biggest unknown in all models based on chlorophyll is how this rate term is
228 described. VGPM considers the primary productivity to be dependent on day length and maxi-
229 mum daily NPP within a water column. The second is Carbon-based Productivity Model (CbPM)
230 which NPP to phytoplankton carbon biomass and growth rate. The third is Carbon, Absorption,
231 and Fluorescence Euphotic-resolving (CAFE) mode; first described by [Silsbe et al., 2016] takes
232 various other factors into NPP calculations. We explore these NPP models and try to explain the
233 variation in zooplankton standing stock.

234 3 The seasonal cycle

235 The previous study of zooplankton in EAS based on ADCP backscatter was consisting of three sites:
236 Mumbai in NEAS, Goa in Central EAS (CEAS) and Kollam in SEAS. The extended mooring sites
237 are at Okha as northernmost in EAS, Jaigarh at CEAS, Udupi in the transition zone of between

238 CEAS & SEAS and Kanyakumari is the southern most site. The seasonal cycle of zooplankton of
239 these seven location is described in this section.

240 **3.1 The seasonal cycle of biomass**

241 A preliminary analysis of the biomass time series in daily and monthly averaged scale shows that
242 the biomass decreases with increasing depth (Fig. 3) at all the seven locations. The high biomass
243 regime in the upper ocean and low biomass regime in deeper depths is differentiated using the 215
244 $mg\ m^{-3}$ biomass contour. For simplicity, this biomass contour is abbreviated to be z215 and its
245 depth is denoted as D215 henceforth; region above this contour is the upper ocean biomass. The
246 choice of 215 $mg\ m^{-3}$ isn't abrupt and carefully chosen to accommodate the seasonal variation, as
247 a shift to biomass contour lower than the z215 would be unviable as our data is only till 120 m
248 depth. A higher biomass contour would lead to inferior view of the seasonal cycle as in the case of
249 Kanyakumari and Okha where D215 is often low enough to reach \sim 20 - 30 m depths. The rate of
250 biomass decrease with depth is highest off Jaigarh and Mumbai as it has higher biomass in upper
251 ocean (Fig. 3,c2,b2). This is followed by central EAS locations Goa and Udupi. While the rate
252 of biomass decrease is lower off Kollam for 2017 to 2020. The rate of decrease is lowest off Okha
253 and Kanyakumari. The rate is roughly defined as the difference between the mean biomass at 40
254 m and 105 m depth. Written in the order of their rate of decrease from the difference of biomass:
255 Jaigarh ($96\ mg\ m^{-3}$), Mumbai ($91\ mg\ m^{-3}$), Okha ($79\ mg\ m^{-3}$), Udupi ($78\ mg\ m^{-3}$), Kollam($73\ mg\ m^{-3}$), Goa ($72\ mg\ m^{-3}$) and Kanyakumari ($39\ mg\ m^{-3}$). The weaker decline in zooplankton
256 biomass with respect to the depth at Okha (Fig. 3.a1,a2) at NEAS is matching with earlier reported
257 data [Madhupratap et al. \[2001\]](#), [Smith and Madhupratap \[2005\]](#), [Wishner et al. \[1998\]](#) where oxygen
258 deficit at is thought to be the cause. The sites at SEAS, especially off Kanyakumari and 2017 to
259 2020

²⁶⁰ 2020 off Kollam also have weaker decline[[Madhupratap et al., 2001](#), [Aparna et al., 2022](#)]. However,
²⁶¹ after 2020 the rate of decline in biomass with depth off Kollam is similar to that off Mumbai in
²⁶² stark contrast to its previous years. This is due to a strong bloom in those years also seen at other
²⁶³ locations(discussed in later section). This high growth led to increase in biomass in the entire water
²⁶⁴ column(Fig. 3.f1,f2).

²⁶⁵ Analysis of the D215 shows strong seasonality at the CEAS moorings off Goa and Jaigarh,
²⁶⁶ with low variation in biomass in its upper ocean, with shallow (deeper) D215 in summer (winter)
²⁶⁷ monsoon. This is followed by the moorings at transition zone off Mumbai (NEAS) and Udupi
²⁶⁸ (SEAS). The

²⁶⁹ include wavelet analysis results

270 make table for the, 40 and 104 mean biomass, the difference, their std **note to self** edit table

271 1

272 **References**

- 273 Anna-Karin Almén and Tobias Tamlander. Temperature-related timing of the spring bloom and match between
274 phytoplankton and zooplankton. *Marine Biology Research*, 16(8-9):674–682, 2020.
- 275 P Amol, D Shankar, V Fernando, A Mukherjee, SG Aparna, R Fernandes, GS Michael, ST Khalap, NP Satelkar,
276 Y Agarvadekar, et al. Observed intraseasonal and seasonal variability of the west india coastal current on the
277 continental slope. *Journal of Earth System Science*, 123(5):1045–1074, 2014.
- 278 P Amol, Suchandan Bemal, D Shankar, V Jain, V Thushara, V Vijith, and PN Vinayachandran. Modulation of
279 chlorophyll concentration by downwelling rossby waves during the winter monsoon in the southeastern arabian
280 sea. *Progress in Oceanography*, 186:102365, 2020.
- 281 SG Aparna, DV Desai, D Shankar, AC Anil, Shrikant Dora, and R Khedekar. Seasonal cycle of zooplankton standing
282 stock inferred from adcp backscatter measurements in the eastern arabian sea. *Progress in Oceanography*, 203:
283 102766, 2022.
- 284 Carin J Ashjian, Sharon L Smith, Charles N Flagg, and Nasseer Idrisi. Distribution, annual cycle, and vertical
285 migration of acoustically derived biomass in the arabian sea during 1994–1995. *Deep Sea Research Part II:*
286 *Topical Studies in Oceanography*, 49(12):2377–2402, 2002.
- 287 K Banse and DC English. Geographical differences in seasonality of czcs-derived phytoplankton pigment in the
288 arabian sea for 1978–1986. *Deep Sea Research Part II: Topical Studies in Oceanography*, 47(7-8):1623–1677, 2000.
- 289 Karl Banse. Hydrography of the arabian sea shelf of india and pakistan and effects on demersal fishes. In *Deep sea*
290 *research and oceanographic Abstracts*, volume 15, pages 45–79. Elsevier, 1968.
- 291 Karl Banse. Zooplankton: pivotal role in the control of ocean production: I. biomass and production. *ICES Journal*
292 *of marine Science*, 52(3-4):265–277, 1995.
- 293 WE Barraclough, RJ LeBrasseur, and OD Kennedy. Shallow scattering layer in the subarctic pacific ocean: detection
294 by high-frequency echo sounder. *Science*, 166(3905):611–613, 1969.
- 295 H. P. Batchelder, J. R. VanKeuren, R. D. Vaillancourt, and E. Swift. Spatial and temporal distributions of acoustically
296 estimated zooplankton biomass near the marine light-mixed layers station (59°30'n, 21°00'w) in the north atlantic
297 in may 1991. *Journal of Geophysical Research: Oceans*, 100:6549–6563, 1995. doi: 10.1029/94jc00981.
- 298 John C Brock and Charles R McClain. Interannual variability in phytoplankton blooms observed in the northwestern
299 arabian sea during the southwest monsoon. *Journal of Geophysical Research: Oceans*, 97(C1):733–750, 1992.
- 300 John C Brock, Charles R McClain, Mark E Luther, and William W Hay. The phytoplankton bloom in the north-
301 western arabian sea during the southwest monsoon of 1979. *Journal of Geophysical Research: Oceans*, 96(C11):
302 20623–20642, 1991.

- 303 Abhisek Chatterjee, D Shankar, SSC Shenoi, GV Reddy, GS Michael, M Ravichandran, VV Gopalkrishna,
304 EP Rama Rao, TVS Udaya Bhaskar, and VN Sanjeevan. A new atlas of temperature and salinity for the north
305 indian ocean. *Journal of Earth System Science*, 121:559–593, 2012.
- 306 Anya Chaudhuri, D Shankar, SG Aparna, P Amol, V Fernando, A Kankonkar, GS Michael, NP Satelkar, ST Khalap,
307 AP Tari, et al. Observed variability of the west india coastal current on the continental slope from 2009–2018.
308 *Journal of Earth System Science*, 129(1):57, 2020.
- 309 Anya Chaudhuri, P Amol, D Shankar, S Mukhopadhyay, SG Aparna, V Fernando, and A Kankonkar. Observed
310 variability of the west india coastal current on the continental shelf from 2010–2017. *Journal of Earth System
311 Science*, 130:1–21, 2021.
- 312 Boris Cisewski, Volker H Strass, Monika Rhein, and Sören Krägesky. Seasonal variation of diel vertical migration
313 of zooplankton from adcp backscatter time series data in the lazarev sea, antarctica. *Deep Sea Research Part I:
314 Oceanographic Research Papers*, 57(1):78–94, 2010.
- 315 Kent L Deines. Backscatter estimation using broadband acoustic doppler current profilers. In *Proceedings of the
316 IEEE Sixth Working Conference on Current Measurement (Cat. No. 99CH36331)*, pages 249–253. IEEE, 1999.
- 317 A Edvardsen, D Slagstad, KS Tande, and P Jaccard. Assessing zooplankton advection in the barents sea using
318 underway measurements and modelling. *Fisheries Oceanography*, 12(2):61–74, 2003.
- 319 S Fielding, G Griffiths, and HSJ Roe. The biological validation of adcp acoustic backscatter through direct comparison
320 with net samples and model predictions based on acoustic-scattering models. *ICES Journal of Marine Science*,
321 61(2):184–200, 2004.
- 322 Charles N Flagg and Sharon L Smith. On the use of the acoustic doppler current profiler to measure zooplankton
323 abundance. *Deep Sea Research Part A. Oceanographic Research Papers*, 36(3):455–474, 1989.
- 324 Kevin D. Friedland, Charles A. Stock, Kenneth F. Drinkwater, Jason S. Link, Robert T. Leaf, Burton Shank, Julie M.
325 Rose, Cynthia H. Pilskaln, and Michael J. Fogarty. Pathways between primary production and fisheries yields of
326 large marine ecosystems, 2012.
- 327 Charles H Greene, Peter H Wiebe, Chris Pelkie, Mark C Benfield, and Jacqueline M Popp. Three-dimensional
328 acoustic visualization of zooplankton patchiness. *Deep Sea Research Part II: Topical Studies in Oceanography*, 45
329 (7):1201–1217, 1998.
- 330 Charles F Greenlaw. Acoustical estimation of zooplankton populations 1. *Limnology and Oceanography*, 24(2):
331 226–242, 1979.
- 332 Davide Guerra, Katrin Schroeder, Mireno Borghini, Elisa Camatti, Marco Pansera, Anna Schroeder, Stefania
333 Sparnocchia, and Jacopo Chiggiato. Zooplankton diel vertical migration in the corsica channel (north-western
334 mediterranean sea) detected by a moored acoustic doppler current profiler. *Ocean Science*, 15(3):631–649, 2019.

- 335 Graeme C Hays. A review of the adaptive significance and ecosystem consequences of zooplankton diel vertical
336 migrations. In *Migrations and Dispersal of Marine Organisms: Proceedings of the 37 th European Marine Biology*
337 *Symposium held in Reykjavik, Iceland, 5–9 August 2002*, pages 163–170. Springer, 2003.
- 338 PJ Herring, MJR Fasham, AR Weeks, JCP Hemmings, HSJ Roe, PR Pugh, S Holley, NA Crisp, and MV Angel.
339 Across-slope relations between the biological populations, the euphotic zone and the oxygen minimum layer off
340 the coast of oman during the southwest monsoon (august, 1994). *Progress in Oceanography*, 41(1):69–109, 1998.
- 341 Karen J Heywood, S Scrope-Howe, and ED Barton. Estimation of zooplankton abundance from shipborne adcp
342 backscatter. *Deep Sea Research Part A. Oceanographic Research Papers*, 38(6):677–691, 1991.
- 343 Laura Hobbs, Neil S Banas, Jonathan H Cohen, Finlo R Cottier, Jørgen Berge, and Øystein Varpe. A marine
344 zooplankton community vertically structured by light across diel to interannual timescales. *Biology Letters*, 17(2):
345 20200810, 2021.
- 346 Raleigh R Hood, Lynnath E Beckley, and Jerry D Wiggert. Biogeochemical and ecological impacts of boundary
347 currents in the indian ocean. *Progress in Oceanography*, 156:290–325, 2017.
- 348 Ryuichiro Inoue, Minoru Kitamura, and Tetsuichi Fujiki. Diel vertical migration of zooplankton at the s 1 biogeo-
349 chemical mooring revealed from acoustic backscattering strength. *Journal of Geophysical Research: Oceans*, 121
350 (2):1031–1050, 2016.
- 351 Songnian Jiang, Tommy D Dickey, Deborah K Steinberg, and Laurence P Madin. Temporal variability of zooplankton
352 biomass from adcp backscatter time series data at the bermuda testbed mooring site. *Deep Sea Research Part I:*
353 *Oceanographic Research Papers*, 54(4):608–636, 2007.
- 354 R Jyothibabu, NV Madhu, H Habeebrehman, KV Jayalakshmy, KKC Nair, and CT Achuthankutty. Re-evaluation
355 of ‘paradox of mesozooplankton’ in the eastern arabian sea based on ship and satellite observations. *Journal of*
356 *Marine Systems*, 81(3):235–251, 2010.
- 357 Myounghee Kang, Sunyoung Oh, Wooseok Oh, Dong-Jin Kang, SungHyun Nam, and Kyounghoon Lee. Acoustic
358 characterization of fish and macroplankton communities in the seychelles-chagos thermocline ridge of the southwest
359 indian ocean. *Deep Sea Research Part II: Topical Studies in Oceanography*, 213:105356, 2024.
- 360 Madhavan Girijakumari Keerthi, Matthieu Lengaigne, Marina Levy, Jerome Vialard, Vallivattathillam Parvathi,
361 Clément de Boyer Montégut, Christian Ethé, Olivier Aumont, Iyyappan Suresh, Valiya Parambil Akhil, et al.
362 Physical control of interannual variations of the winter chlorophyll bloom in the northern arabian sea. *Biogeosciences*, 14(15):3615–3632, 2017.
- 364 Corinne Le Qu, Robbie M Andrew, Josep G Canadell, Stephen Sitch, Jan Ivar Korsbakken, Glen P Peters, Andrew C
365 Manning, Thomas A Boden, Pieter P Tans, Richard A Houghton, et al. Global carbon budget 2016. *Earth System*
366 *Science Data*, 8(2):605–649, 2016.

- 367 Marina Lévy, D Shankar, J-M André, SSC Shenoi, Fabien Durand, and Clément de Boyer Montégut. Basin-wide
368 seasonal evolution of the indian ocean's phytoplankton blooms. *Journal of Geophysical Research: Oceans*, 112
369 (C12), 2007.
- 370 M Li, A Gargett, and K Denman. What determines seasonal and interannual variability of phytoplankton and
371 zooplankton in strongly estuarine systems? *Estuarine, Coastal and Shelf Science*, 50(4):467–488, 2000.
- 372 Yanliang Liu, Jingsong Guo, Yuhuan Xue, Chalermrat Sangmanee, Huiwu Wang, Chang Zhao, Somkiat Khokiat-
373 tiwong, and Weidong Yu. Seasonal variation in diel vertical migration of zooplankton and micronekton in the
374 andaman sea observed by a moored adcp. *Deep Sea Research Part I: Oceanographic Research Papers*, 179:103663,
375 2022.
- 376 M Madhupratap, P Haridas, Neelam Ramaiah, and CT Achuthankutty. Zooplankton of the southwest coast of india:
377 abundance, composition, temporal and spatial variability in 1987. 1992.
- 378 M Madhupratap, TC Gopalakrishnan, P Haridas, KKC Nair, PN Aravindakshan, G Padmavati, and Shiney Paul.
379 Lack of seasonal and geographic variation in mesozooplankton biomass in the arabian sea and its structure in the
380 mixed layer. *Current science. Bangalore*, 71(11):863–868, 1996a.
- 381 M Madhupratap, S Prasanna Kumar, PMA Bhattachari, M Dileep Kumar, S Raghukumar, KKC Nair, and N Rama-
382 iah. Mechanism of the biological response to winter cooling in the northeastern arabian sea. *Nature*, 384(6609):
383 549–552, 1996b.
- 384 M Madhupratap, TC Gopalakrishnan, P Haridas, and KKC Nair. Mesozooplankton biomass, composition and
385 distribution in the arabian sea during the fall intermonsoon: implications of oxygen gradients. *Deep Sea Research
386 Part II: Topical Studies in Oceanography*, 48(6-7):1345–1368, 2001.
- 387 PA Maheswaran, G Rajesh, C Revichandran, and KKC Nair. Upwelling and associated hydrography along the west
388 coast of india during southwest monsoon, 1999. 2000.
- 389 JP McCreary, Raghu Murtugudde, Jerome Vialard, PN Vinayachandran, Jerry D Wiggert, Raleigh R Hood,
390 D Shankar, and S Shetye. Biophysical processes in the indian ocean. *Indian Ocean biogeochemical processes
391 and ecological variability*, 185:9–32, 2009.
- 392 Julian P McCreary Jr, Pijush K Kundu, and Robert L Molinari. A numerical investigation of dynamics, thermody-
393 namics and mixed-layer processes in the indian ocean. *Progress in Oceanography*, 31(3):181–244, 1993.
- 394 Donald C McNaught. Acoustical determination of zooplankton distribution. In *Proc. 11th Conf. Great lakes Res.*,
395 pages 76–84, 1968.
- 396 A Mukherjee, D Shankar, V Fernando, P Amol, SG Aparna, R Fernandes, GS Michael, ST Khalap, NP Satelkar,
397 Y Agarvadekar, et al. Observed seasonal and intraseasonal variability of the east india coastal current on the
398 continental slope. *Journal of Earth System Science*, 123(6):1197–1232, 2014.

- 399 S Mukhopadhyay, D Shankar, SG Aparna, A Mukherjee, V Fernando, A Kankonkar, S Khalap, NP Satelkar,
400 MG Gaonkar, AP Tari, et al. Observed variability of the east india coastal current on the continental slope
401 during 2009–2018. *Journal of Earth System Science*, 129:1–22, 2020.
- 402 Jerry Mullison. Backscatter estimation using broadband acoustic doppler current profilers-updated. In *Proceedings*
403 *of the ASCE Hydraulic Measurements & Experimental Methods Conference, Durham, NH, USA*, pages 9–12,
404 2017.
- 405 KKC Nair, M Madhupratap, TC Gopalakrishnan, P Haridas, and Mangesh Gauns. The arabian sea: physical
406 environment, zooplankton and myctophid abundance. 1999.
- 407 PV Nair. Primary productivity in the indian seas. *CMFRI Bulletin*, 22:1–63, 1970.
- 408 Lingyun Nie, Jianchao Li, Hao Wu, Wenchao Zhang, Yongjun Tian, Yang Liu, Peng Sun, Zhenjiang Ye, Shuyang
409 Ma, and Qinfeng Gao. The influence of ocean processes on fine-scale changes in the yellow sea cold water mass
410 boundary area structure based on acoustic observations. *Remote Sensing*, 15(17):4272, 2023.
- 411 MD Ohman and H-J Hirche. Density-dependent mortality in an oceanic copepod population. *Nature*, 412(6847):
412 638–641, 2001.
- 413 G Padmavati, P Haridas, KKC Nair, TC Gopalakrishnan, P Shiney, and M Madhupratap. Vertical distribution of
414 mesozooplankton in the central and eastern arabian sea during the winter monsoon. *Journal of Plankton Research*,
415 20(2):343–354, 1998.
- 416 MR Patil, CP Ramamirtham, P Udaya Varma, and CP Nair. Hydrography of the west coast of india during the
417 pre-monsoon period of the year 1962. *Journal of marine biological association of India*, 6(1):151–164, 1964.
- 418 Richard Edward Pieper. *A study of the relationship between zooplankton and high-frequency scattering of underwater*
419 *sound*. PhD thesis, University of British Columbia, 1971.
- 420 SA Piontковски, R Williams, and TA Melnik. Spatial heterogeneity, biomass and size structure of plankton of the
421 indian ocean: some general trends. *Marine ecology progress series*, pages 219–227, 1995.
- 422 Emmanuel Potiris, Constantin Frangoulis, Alkiviadis Kalampokis, Manolis Ntoumas, Manos Pettas, George Peti-
423 hakis, and Vassilis Zervakis. Acoustic doppler current profiler observations of migration patterns of zooplankton
424 in the cretan sea. *Ocean Science*, 14(4):783–800, 2018.
- 425 SZ Qasim. Biological productivity of the indian ocean. 1977.
- 426 CP Ramamirtham and AVS Murty. Hydrography of the west coast of india during the pre-monsoon period of the
427 year 1962—part 2: in and offshore waters of the konkan and malabar coasts. *Journal of the Marine Biological*
428 *Association of India*, 7(1):150–168, 1965.
- 429 S Ramamurthy. Studies on the plankton of the north kanara coast in relation to the pelagic fishery. *Journal of*
430 *Marine Biological Association of India*, 7(1):127–149, 1965.

- 431 Mehbuba Rehim and Mudassar Imran. Dynamical analysis of a delay model of phytoplankton–zooplankton interac-
432 tion. *Applied Mathematical Modelling*, 36(2):638–647, 2012.
- 433 T. P. Rippeth and J. H. Simpson. Diurnal signals in vertical motions on the hebridean shelf. *Limnology and*
434 *Oceanography*, 43:1690–1696, 1998. doi: 10.4319/lo.1998.43.7.1690.
- 435 John H Ryther, John R Hall, Allan K Pease, Andrew Bakun, and Mark M Jones. Primary organic production in
436 relation to the chemistry and hydrography of the western indian ocean 1. *Limnology and Oceanography*, 11(3):
437 371–380, 1966.
- 438 D Sameoto and S Paulowich. The use of 120 khz sonar in zooplankton studies. In *OCEANS'77 Conference Record*,
439 pages 523–528. IEEE, 1977.
- 440 D Shankar and SR Shetye. On the dynamics of the lakshadweep high and low in the southeastern arabian sea.
441 *Journal of Geophysical Research: Oceans*, 102(C6):12551–12562, 1997.
- 442 D Shankar, R Remya, PN Vinayachandran, Abhisek Chatterjee, and Ambica Behera. Inhibition of mixed-layer
443 deepening during winter in the northeastern arabian sea by the west india coastal current. *Climate Dynamics*,
444 47:1049–1072, 2016.
- 445 D Shankar, R Remya, AC Anil, and V Vijith. Role of physical processes in determining the nature of fisheries in the
446 eastern arabian sea. *Progress in Oceanography*, 172:124–158, 2019.
- 447 SR Shetye and AD Gouveia. Coastal circulation in the north indian ocean: Coastal segment (14, sw). John Wiley
448 and Sons, New York, USA, 1998.
- 449 SR Shetye, AD Gouveia, SSC Shenoi, GS Michael, D Sundar, AM Almeida, and K Santanam. The coastal current
450 off western india during the northeast monsoon. *Deep Sea Research Part A. Oceanographic Research Papers*, 38
451 (12):1517–1529, 1991.
- 452 SR Shetye, AD Gouveia, and SSC Shenoi. Does winter cooling lead to the subsurface salinity minimum off saurashtra,
453 india? *Oceanography of the Indian Ocean*, pages 617–625, 1992.
- 454 Greg M Silsbe, Michael J Behrenfeld, Kimberly H Halsey, Allen J Milligan, and Toby K Westberry. The cafe model:
455 A net production model for global ocean phytoplankton. *Global Biogeochemical Cycles*, 30(12):1756–1777, 2016.
- 456 Houssem Smeti, Marc Pagano, Christophe Menkes, Anne Lebourges-Dhaussy, Brian PV Hunt, Valerie Allain, Martine
457 Rodier, Florian De Boissieu, Elodie Kestenare, and Cherif Sammari. Spatial and temporal variability of zooplank-
458 ton off n ew c aledonia (s outhwestern p acific) from acoustics and net measurements. *Journal of Geophysical*
459 *Research: Oceans*, 120(4):2676–2700, 2015.
- 460 SL Smith and M Madhupratap. Mesozooplankton of the arabian sea: patterns influenced by seasons, upwelling, and
461 oxygen concentrations. *Progress in Oceanography*, 65(2-4):214–239, 2005.

- 462 R Subrahmanyam. Studies on the phytoplankton of the west coast of india: Part ii. physical and chemical factors
463 influencing the production of phytoplankton, with remarks on the cycle of nutrients and on the relationship of
464 the phosphate-content to fish landings. In *Proceedings/Indian Academy of Sciences*, volume 50, pages 189–252.
465 Springer, 1959.
- 466 R Subrahmanyam and AH Sarma. Studies on the phytoplankton of the west coast of india. part iii. seasonal variation
467 of the phytoplankters and environmental factors. *Indian Journal of Fisheries*, 7(2):307–336, 1960.
- 468 Laura Ursella, Vanessa Cardin, Mirna Batistić, Rade Garić, and Miroslav Gačić. Evidence of zooplankton vertical
469 migration from continuous southern adriatic buoy current-meter records. *Progress in oceanography*, 167:78–96,
470 2018.
- 471 Laura Ursella, Sara Pensieri, Enric Pallàs-Sanz, Sharon Z Herzka, Roberto Bozzano, Miguel Tenreiro, Vanessa Cardin,
472 Julio Candela, and Julio Sheinbaum. Diel, lunar and seasonal vertical migration in the deep western gulf of mexico
473 evidenced from a long-term data series of acoustic backscatter. *Progress in Oceanography*, 195:102562, 2021.
- 474 V Vijith, PN Vinayachandran, V Thushara, P Amol, D Shankar, and AC Anil. Consequences of inhibition of mixed-
475 layer deepening by the west india coastal current for winter phytoplankton bloom in the northeastern arabian sea.
476 *Journal of Geophysical Research: Oceans*, 121(9):6583–6603, 2016.
- 477 Peter H Wiebe, Charles H Greene, Timothy K Stanton, and Janusz Burczynski. Sound scattering by live zooplankton
478 and micronekton: empirical studies with a dual-beam acoustical system. *The Journal of the Acoustical Society of
479 America*, 88(5):2346–2360, 1990.
- 480 Monika Winder and Daniel E Schindler. Climatic effects on the phenology of lake processes. *Global change biology*,
481 10(11):1844–1856, 2004.
- 482 Karen F Wishner, Marcia M Gowing, and Celia Gelfman. Mesozooplankton biomass in the upper 1000 m in the
483 arabian sea: overall seasonal and geographic patterns, and relationship to oxygen gradients. *Deep Sea Research
484 Part II: Topical Studies in Oceanography*, 45(10-11):2405–2432, 1998.

Table 1: ADCP deployment details at the locations. The temporal resolution is 1 hour, bin size(vertical resolution) 4 m. All ADCPs are operated at 153.3 kHz. The moorings are at a water column depth of 950 - 1200 m on the continental slope and are serviced on yearly basis according to ship availability. The 6th column consists of Reference echo intensity (Er) for each beam, while the 7th column contains the corresponding RSSI conversion factor [Deines, 1999].

Station (Position; $^{\circ}$ E, $^{\circ}$ N)	Date		Depth			
	Deployment	Recovery	Ocean	ADCP	Er	Kc
Okha (67.47, 22.26)	01/10/2018	01/12/2019	996	118	37 , 37 , 37 , 36	0.42 , 0.44 , 0.42 , 0.43
	01/12/2019	04/12/2020	1166	312	39 , 36 , 38 , 36	0.42 , 0.44 , 0.42 , 0.43
	04/12/2020	08/03/2022	1021	144	41 , 37 , 38 , 37	0.42 , 0.44 , 0.42 , 0.43
	08/03/2022	01/01/2023	1019	142	37 , 38 , 39 , 36	0.42 , 0.44 , 0.42 , 0.43
Mumbai (69.24, 20.01)	09/11/2017	29/09/2018	1025	150	36 , 34 , 39 , 42	0.40 , 0.40 , 0.40 , 0.40
	29/09/2018	29/11/2019	1122	125	35 , 36 , 39 , 42	0.40 , 0.40 , 0.40 , 0.40
	29/11/2019	02/12/2020	1143	164	37 , 34 , 39 , 43	0.40 , 0.40 , 0.40 , 0.40
	02/12/2020	06/03/2022	1125	142	36 , 34 , 39 , 42	0.40 , 0.40 , 0.40 , 0.40
	07/03/2022	02/01/2023	1103	158	37 , 34 , 40 , 43	0.40 , 0.40 , 0.40 , 0.40
Jaigarh (71.12, 17.53)	27/10/2017	27/09/2018	1039	198	32 , 35 , 33 , 32	0.45 , 0.45 , 0.45 , 0.45
	27/09/2018	30/10/2019	1032	164	32 , 35 , 33 , 31	0.45 , 0.45 , 0.45 , 0.45
	03/11/2019	30/11/2020	1142	264	32 , 36 , 33 , 32	0.45 , 0.45 , 0.45 , 0.45
	30/11/2020	05/03/2022	1099	119	33 , 36 , 34 , 32	0.45 , 0.45 , 0.45 , 0.45
	03/04/2022	26/06/2022	1120	136	68 , 71 , 69 , 66	0.45 , 0.45 , 0.45 , 0.45
Goa (72.74, 15.17)	03/10/2017	25/09/2018	1000	174	35 , 37 , 34 , 35	0.44 , 0.44 , 0.40 , 0.41
	25/09/2018	16/10/2019	969	145	38 , 36 , 36 , 34	0.44 , 0.44 , 0.40 , 0.41
	16/10/2019	29/11/2020	966	143	44 , 38 , 36 , 43	0.44 , 0.44 , 0.40 , 0.41
	29/11/2020	03/03/2022	985	157	35 , 40 , 35 , 38	0.44 , 0.44 , 0.40 , 0.41
	03/03/2022	05/01/2023	984	159	35 , 38 , 35 , 34	0.44 , 0.44 , 0.40 , 0.41
Udupi (74.04, 12.5)	05/10/2017	06/10/2018	1028	176	44 , 46 , 29 , 35	0.45 , 0.45 , 0.45 , 0.45
	06/10/2018	18/10/2019	1027	179	32 , 38 , 30 , 36	0.45 , 0.45 , 0.45 , 0.45
	18/10/2019	11/12/2020	1018	168	33 , 37 , 31 , 38	0.45 , 0.45 , 0.45 , 0.45
	11/03/2022	06/01/2023	1036	155	31 , 32 , 32 , 33	0.45 , 0.45 , 0.45 , 0.45
Kollam (75.44, 9.05)	07/10/2017	08/10/2018	1174	200	43 , 55 , 45 , 43	0.49 , 0.50 , 0.49 , 0.50
	08/10/2018	20/10/2019	1160	123	49 , 62 , 46 , 46	0.49 , 0.50 , 0.49 , 0.50
	20/10/2019	13/12/2020	1209	176	52 , 61 , 54 , 55	0.49 , 0.50 , 0.49 , 0.50
	13/12/2020	13/03/2022	1129	91	49 , 51 , 46 , 47	0.49 , 0.50 , 0.49 , 0.50
	13/03/2022	08/01/2023	1149	164	41 , 48 , 43 , 41	0.49 , 0.50 , 0.49 , 0.50
Kanyakumari (77.39, 6.96)	16/11/2016	08/10/2017	1096	252	37 , 36 , 37 , 37	0.42 , 0.44 , 0.42 , 0.43
	08/10/2017	10/10/2018	1055	181	32 , 34 , 38 , 35	0.45 , 0.45 , 0.45 , 0.45
	10/10/2018	22/10/2019	1075	180	36 , 34 , 39 , 36	0.45 , 0.45 , 0.45 , 0.45
	22/10/2019	14/12/2020	1060	167	33 , 35 , 36 , 35	0.45 , 0.45 , 0.45 , 0.45
	14/12/2020	14/03/2022	1184	287	34 , 36 , 36 , 35	0.45 , 0.45 , 0.45 , 0.45
	14/03/2022	10/01/2023	1069	172	33 , 36 , 42 , 36	0.45 , 0.45 , 0.45 , 0.45

Table 2:
Volumetric samples of zooplankton of various stations. The tags corresponds to cruise and particular station. The sampling depth range is standardised for later years for bin range of 0-25m, 25-50m, 50-75m, 75-100m, 100-150m

Sample number	Tag	Lat($^{\circ}$ N)	Lon($^{\circ}$ E)	Date	Time (IST)	Sampling depth range (m)
1-3	G1	15.18	72.79	25 Sep 18	452	50–25, 100–50, 150–100
4-6	G2	15.16	72.71	25 Sep 18	2108	50–25, 100–50, 150–100
7-10	G2	15.16	72.71	25 Sep 18	2137	40–20, 60–40, 80–60, 100–80
11-14	J1			26 Sep 18	2000	40–20, 60–40, 80–60, 100–80
15-17	J2			27 Sep 18	2000	50–25, 100–50, 150–100
18-21	J2			27 Sep 18	2100	40–20, 60–40, 80–60, 100–80
22-25	M1	20	69.19	28 Sep 18	2135	40–20, 60–40, 80–60, 100–80
26-27	M1	20	69.19	28 Sep 18	2205	50–25, 100–50
28-29	M2	20.01	69.2	29 Sep 18	2035	50–25, 100–50
30-33	M2	20.01	69.2	29 Sep 18	2057	40–20, 60–40, 80–60, 100–80
34-37	U1			5 Oct 18	2000	40–20, 60–40, 80–60, 100–80
38-40	U1			5 Oct 18	2100	50–25, 100–50, 150–100
41-43	U2			6 Oct 18	2000	50–25, 100–50, 150–100
44-47	U2			6 Oct 18	2100	40–20, 60–40, 80–60, 100–80
48-51	K1	9.06	75.42	8 Oct 18	421	40–20, 60–40, 80–60, 100–80
52-54	K1	9.06	75.42	8 Oct 18	449	50–25, 100–50, 150–100
55-56	K2	9.04	75.4	8 Oct 18	2027	50–25, 100–50
57-60	K2	9.04	75.4	8 Oct 18	2045	40–20, 60–40, 80–60, 100–80
61-64	G2	15.16	72.74	16 Oct 19	829	50–25, 75–50, 100–75, 150–100
65-67	G3	15.16	72.74	16 Oct 19	1812	50–25, 75–50, 100–75
68-70	K2	9.02	75.42	20 Oct 19	840	50–25, 75–50, 100–75
71-74	K3	9.04	75.43	20 Oct 19	1934	50–25, 75–50, 100–75, 150–100
75-78	KK1			22 Oct 19	742	50–25, 75–50, 100–75, 150–100
79-82	KK2			22 Oct 19	1925	50–25, 75–50, 100–75, 150–100
83-86	J1			30 Oct 19	324	50–25, 75–50, 100–75, 150–100
87-89	J2			4 Nov 19	946	75–50, 100–75, 150–100
90-92	M2	19.98	69.22	29 Nov 19	1434	50–25, 75–50, 100–75
93-96	M3	20.01	69.23	30 Nov 19	958	50–25, 75–50, 100–75, 150–100
97-100	O1	22.24	67.49	1 Dec 19	937	50–25, 75–50, 100–75, 150–100
101	O2	22.25	67.46	1 Dec 19	1957	150-100
102-105	G3	15.68	73.22	28 Nov 20	930	50–25, 75–50, 100–75, 150–100
105-108	G4	15.32	73.22	29 Nov 20	1558	50–25, 75–50, 100–75, 150–100
108-110	J2	17.85	71.21	30 Nov 20	1458	75–50, 100–75, 150–100
111-114	J3	17.91	71.21	1 Dec 20	1052	50–25, 75–50, 100–75, 150–100
115-118	M4	20.03	69.38	2 Dec 20	2016	50–25, 75–50, 100–75, 150–100
119-00	O2	22.41	67.8	4 Dec 20	953	150-100
120-123	O3	22.41	67.79	4 Dec 20	2011	50–25, 75–50, 100–75, 150–100
124-127	K3	9.11	75.72	12 Dec 20	2335	50–25, 75–50, 100–75, 150–100
128-131	K4	9.06	75.74	13 Dec 20	1507	50–25, 75–50, 100–75, 150–100
132-134	KK1	7.62	77.63	14 Dec 20	1226	50–25, 75–50
135-138	KK2	7.62	77.63	14 Dec 20	2047	50–25, 75–50, 100–75, 150–100
139-142	G4	15.32	73.21	3 Mar 22	823	50–25, 75–50, 100–75, 150–100
143-146	G5	15.68	73.21	4 Mar 22	1030	50–25, 75–50, 100–75, 150–100
147-150	M5	19.99	69.23	7 Mar 22	957	50–25, 75–50, 100–75, 150–100
151-154	O3	22.24	67.5	8 Mar 22	806	50–25, 75–50, 100–75, 150–100
155-158	U3	12.5	74.04	12 Mar 22	1156	50–25, 75–50, 100–75, 150–100
159-160	K4	9.04	75.42	13 Mar 22	1027	50–25, 75–50, 100–75
161-164	KK3	6.97	77.4	15 Mar 22	1220	50–25, 75–50, 100–75, 150–100

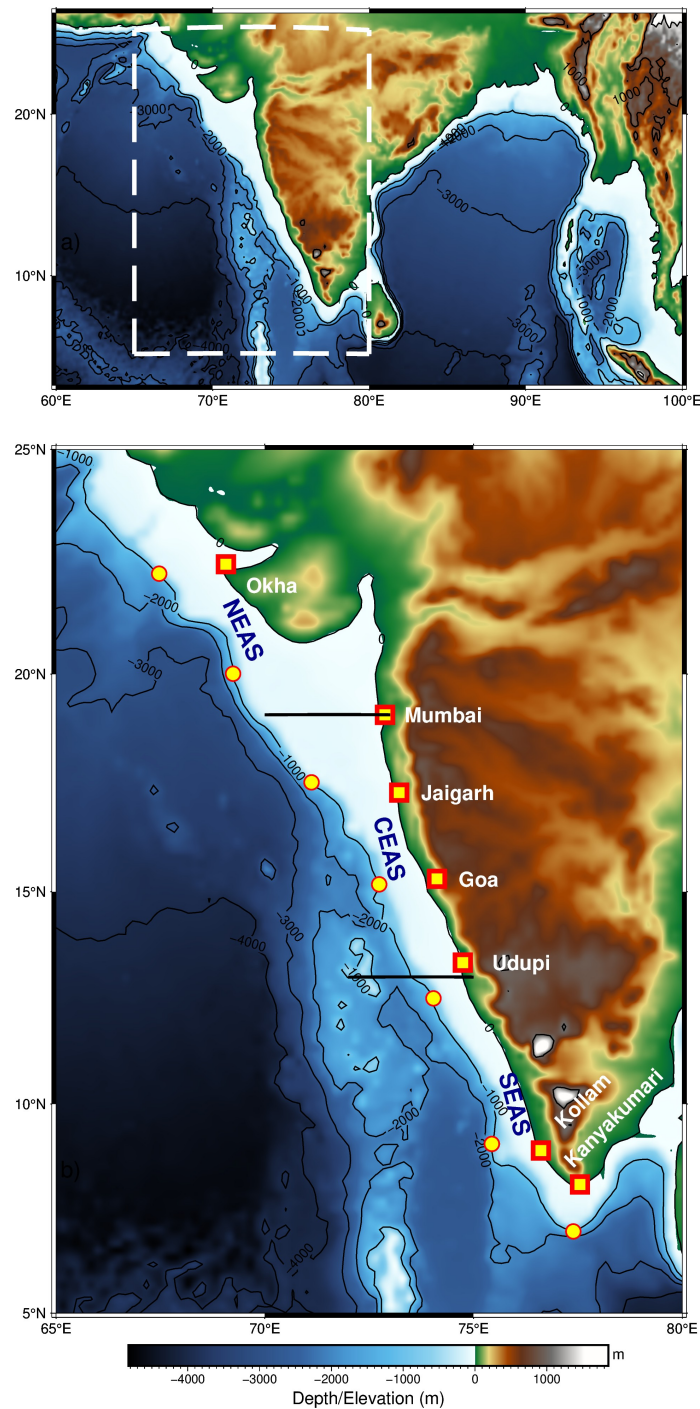


Figure 1: Map showing region of interest. The slope moorings are deployed at 1000 m depth.

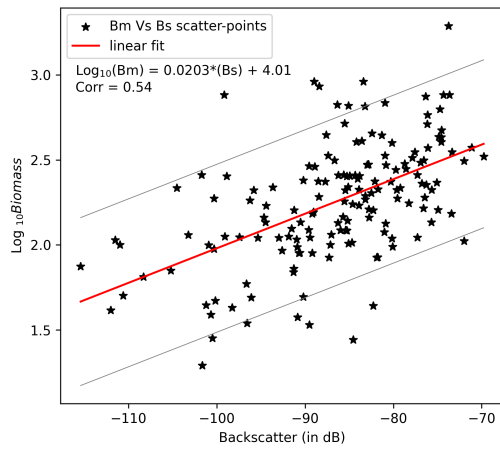


Figure 2: The linear fit line of Biomass (taken in log of biomass) and Backscatter. The linear fit line is within the error range of previous result of [Aparna et al., 2022] onto which latest zooplankton volumetric sample data is added.

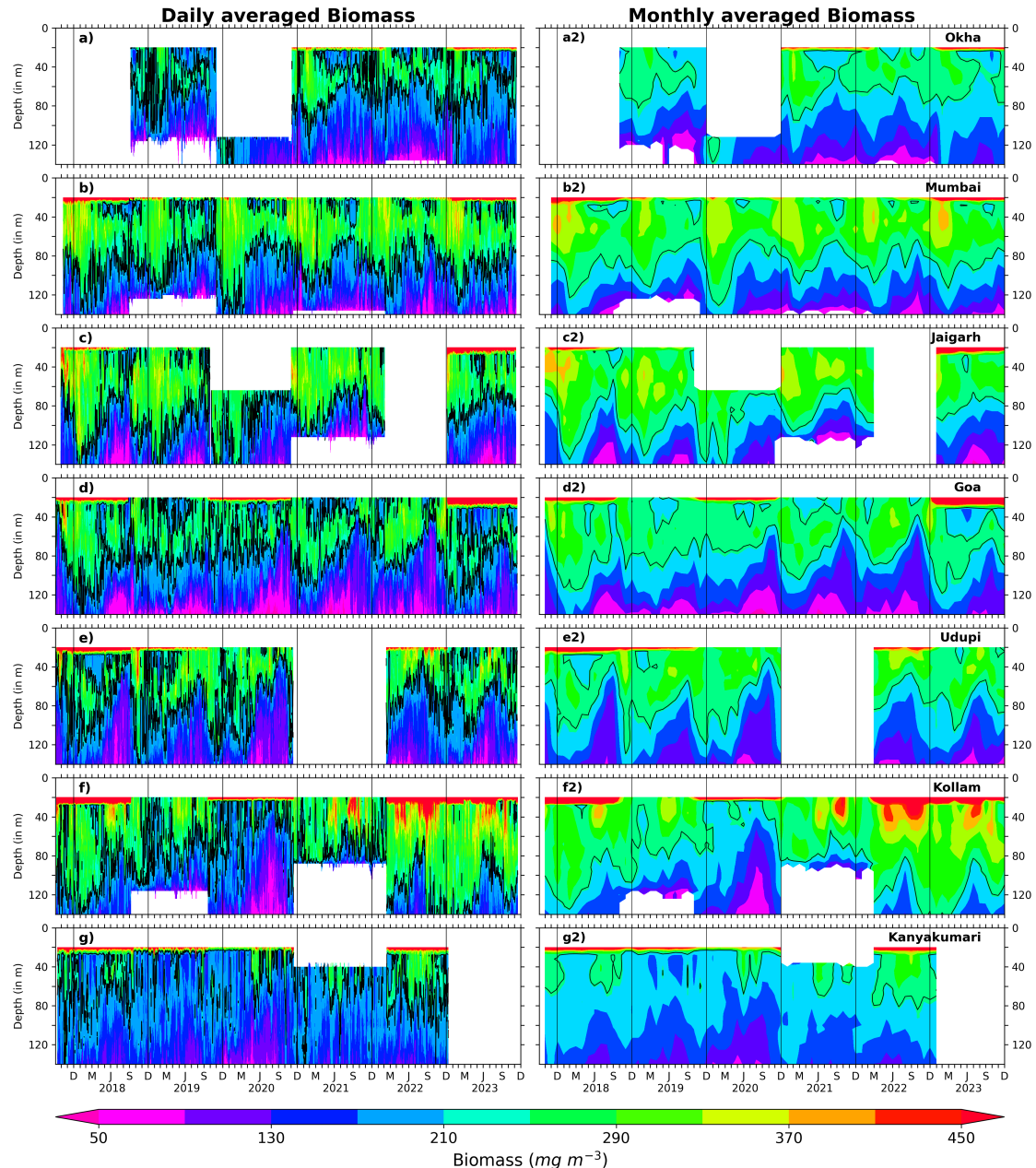


Figure 3: The Daily and monthly averaged biomass for EAS moorings, north (top) to south (bottom). The black contours are marking 215 mg m^{-3} biomass.

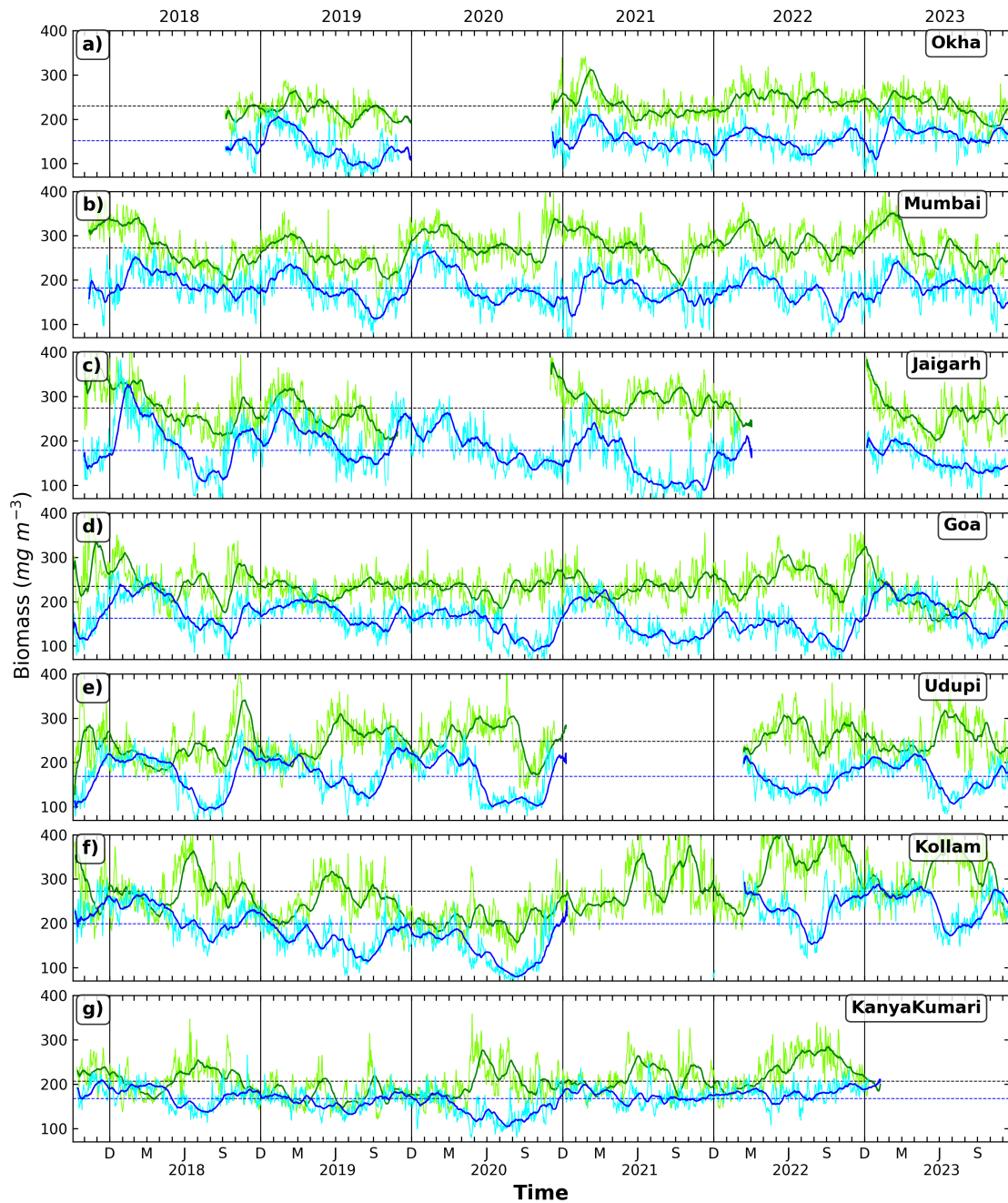


Figure 4: The daily biomass at depth of 40 m and 104 m for all locations shown by grey and cyan curves. The black and blue lines shows the 30 day rolling averaged biomass.

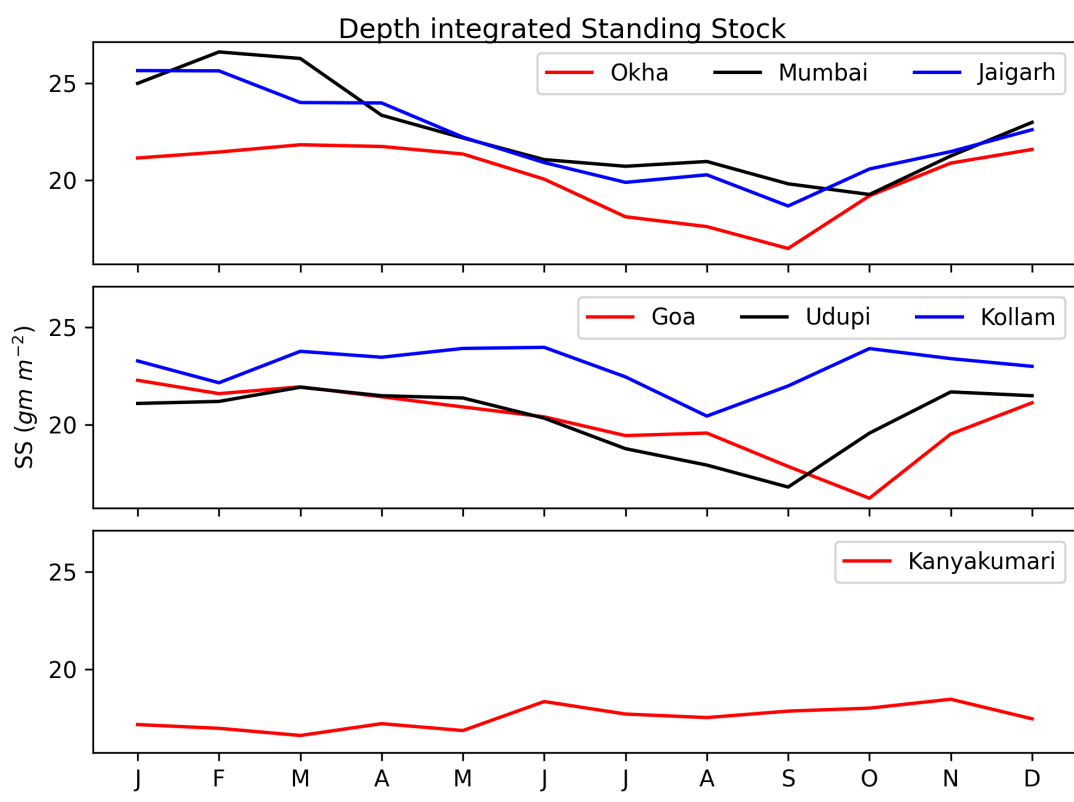


Figure 5